Generation of Nonminimum Phase From Amplitude-Only Data

Tapan K. Sarkar, *Fellow, IEEE,* and Bin Hu

***Abstract*—A method is presented for the generation of nonminimum phase from amplitude-only data. The nonminimum phase is generated utilizing the principles of causality and the Hilbert transform. The application of the theory has been applied to some antenna radiation-power patterns and to measured transfer functions of microwave filters to illustrate the applicability of this approach.**

***Index Terms*— Amplitude-only, Hilbert transform, nonminimum phase.**

I. Introduction

RECONSTRUCTION of phase from amplitude-only data is an important problem. For minimum phase systems, the reconstruction of phase from amplitude-only data is relatively straightforward as the phase response is given by the Hilbert transform of the log of the magnitude of the amplitude data [1]–[3]. In other words, the minimum phase as a function of frequency w is given by $\arg[X(w)]$ and is expressed as

$$\arg[X(w)] = -\frac{1}{\pi} P \int_{-\infty}^{\infty} \frac{\ln|X(\lambda)|}{\lambda - w}\, d\lambda \tag{1}$$

where P denotes a principal-value integral, as the integrand has a singularity and is not integrable. The integral in (1) only exists in a principal-value sense. However, this property given by (1) of a linear-time invariant system does not hold if the system is not minimum phase. The minimum-phase property of a transfer function $X(w)$ refers only to all the zeros of $X(s)$. The zeros must lie in the left half ($s = \sigma + jw$ with $\sigma < 0$) of the s-plane. If the system is not minimum phase (i.e., when some of the zeros of the transfer function may be on the right half-plane), then (1) does not hold. Most electromagnetic systems have a nonminimum phase response. Hence, (1) has very little use for the practical problems. However, there is a more general result of the Hilbert transform, which is based on causality. This result is valid for a nonminimum phase system. We utilize the principle of causality to do nonminimum phase realizations. The principle of causality implies that the function $f(t) = 0$ for $t < 0$ and is nonzero otherwise. It is important at the onset to point out that the phase realization (be it minimum or nonminimum phase) is not a unique problem. A linear-phase term may be added to any phase function without altering its amplitude spectrum. This is because the addition of a linear phase to the phase of the transfer function with a uniform amplitude is equivalent to a pure delay in the time domain. Since we are dealing with linear-shift invariant systems (as the response of the system is the same independent of the time origin), changing the impulse response of the system by a time shift does not alter the transfer function of the original system, except that the phase spectrum is modified by a linear-phase function. The slope of this linear-phase function is equivalent to the time delay. Also, the amplitude spectrum of the transfer function is unaltered by providing a delay to the impulse response of the system at hand.

In Section II, we present the more general amplitude–phase relationship of a nonminimum phase system based on the principles of causality. In Section III, the computational method is outlined. In Section IV, we describe the numerical implementation of this technique. Section V describes how this technique can be applied for the realization of nonminimum phase from the field power patterns. Typical numerical results are presented in Section VI, followed by a conclusion in Section VII.

II. Properties of Transfer Functions Based on Causality

A function $x(t)$ is said to be "causal" if

$$x(t) = 0, \qquad \text{whenever } t < 0. \tag{2}$$

These type of functions arise in the study of causal systems and are of obvious importance in describing phenomena that have well-defined "starting points."

Let $x(t)$ be a real causal function with Fourier transform $X(w)$, and let $R(w)$ and $I(w)$ be the real and imaginary parts of $X(w)$. Then,

$$X(w) = R(w) + jI(w) = |X(w)|e^{j\phi(w)}. \tag{3}$$

Since $x(t)$ is real, $R(w)$ is even and $I(w)$ is odd as a function of w. A general question of whether a particular amplitude characteristic can be realized as a causal system is answered by the Paley–Wiener criterion. Consider a specific magnitude of a transfer function $|X(w)|$. It can be realized by means of a causal system if and only if the integral

$$\int_{-\infty}^{\infty} \frac{\ln|X(w)|}{1+w^2}\, dw < \infty \tag{4}$$

is bounded. Then, a phase function associated with $|X(w)|$ exists such that the impulse response $x(t)$ is causal. The Paley–Wiener criterion is satisfied only if the support of

Manuscript received February 10, 1997; revised May 11, 1998. This work was supported in part by the Office of Naval Research under Contract N00014-98-1-0279.

The authors are with the Department of Electrical Engineering and Computer Engineering, Syracuse University, Syracuse, NY 13244-1240 USA.

Publisher Item Identifier S 0018-9480(98)05513-6.

$|X(w)|$ is unbounded. Otherwise, $|X(w)|$ would be equal to zero over finite intervals of frequency, and this would result in infinite values of the $\ln|X(w)| = \infty$.

Provided $X(w)$ has a causal representation, one can write [4]

$$x(t) = \frac{2}{\pi}\int_0^\infty R(w)\cos wt\, dw, \qquad 0 < t \tag{5}$$

$$x(t) = -\frac{2}{\pi}\int_0^\infty I(w)\sin wt\, dw, \qquad 0 < t \tag{6}$$

and also,

$$\int_0^\infty |x(t)|^2\, dt = \frac{1}{\pi}\int_{-\infty}^\infty |R(w)|^2\, dw = \frac{1}{\pi}\int_{-\infty}^\infty |I(w)|^2\, dw. \tag{7}$$

In addition, if $x(t)$ is bounded at the origin, then we have

$$R(w) = -\frac{1}{\pi}\int_{-\infty}^\infty \frac{I(s)}{w-s}\, ds = -\mathcal{H}[I(w)] \tag{8}$$

$$I(w) = \frac{1}{\pi}\int_{-\infty}^\infty \frac{R(s)}{w-s}\, ds = \mathcal{H}[R(w)]. \tag{9}$$

Here, the symbol $\mathcal{H}[\cdot]$ defines the Hilbert transform. It constitutes a convolution operation with the function $1/\pi w$, which is not defined at $w = 0$. Hence, both (8) and (9) have to be interpreted in the principal-value sense. The last two integrals are defined in terms of the Hilbert transforms and has been defined using Cauchy principal values. Note that (8) and (9) hold for nonminimum phase systems. The only restriction is that $x(t)$ be causal. This restriction holds for most practical systems.

III. Application of the Principles of Hilbert Transform for Phase Recovery

The analysis of the previous sections define the transfer function $R(w) + jI(w)$ over the infinite angular frequency interval $-\infty < w < \infty$. However, in practice, $R(w)$ and $I(w)$ is specified only over a finite segment. Hence, the analysis of the Section II is modified. The modification is carried out by assuming $R(w)$ and $I(w)$ as periodic functions and are denoted by $R_p(w)$ and $I_p(w)$. For computational reasons, this is done as illustrated in [5]. We have earlier carried out computations using those principles of [5] in [6]. Under that assumption, since $R_p(w)$ is even with a period of 2π from $-\pi$ to π, one can write

$$R_p(w) = a_0 + \sum_{n=1}^\infty a_n \cos(nw + \phi_n), \qquad \text{for } 0 < w < \pi \tag{10}$$

where a_i for $i = 0, \cdots, \infty$ are the discrete Fourier cosine transform of $R(w)$ in the half-period π. ϕ_n are certain phases associated with the coefficients a_n. The number of terms of the cosine series may be finite or infinite. However, for numerical computations, we take a finite number of terms of the series and, thus, the upper limit of the summation is replaced by N.

By taking the Hilbert transform of (10), one obtains from (8)

$$\begin{aligned} I_p(w) &= \mathcal{H}[R_p(w)] \\ &= -\sum_{n=1}^\infty a_n \sin(nw + \phi_n), \qquad \text{for } 0 < w < \pi. \end{aligned} \tag{11}$$

The point to make here is that the same Fourier coefficients that are used in (10) are also being used in (11), so that (10) and (11) are related through the coefficients a_i and ϕ_i.

Now, if we are given the magnitude response of the system, i.e., power spectrum, then

$$\begin{aligned} |X(w)|^2 &= |R(w)|^2 + |I(w)|^2 \\ &\simeq |R_p(w)|^2 + |I_p(w)|^2, \qquad \text{for } 0 < w < \pi \\ &= \left| a_0 + \sum_{n=1}^\infty a_n \cos(nw + \phi_n) \right|^2 \\ &\quad + \left| \sum_{n=1}^\infty a_n \sin(nw + \phi_n) \right|^2. \end{aligned} \tag{12}$$

Now, given the power spectrum of the system, i.e., given $|X(w)|^2$ for $0 < w < \pi$, then one can now utilize an optimization routine to solve for the a_i's and ϕ_i's to minimize the error function $E(w)$ given by

$$\begin{aligned} E(w) = \Bigg[|X(w)|^2 &- \left| a_0 + \sum_{n=1}^\infty a_n \cos(nw + \phi_n) \right|^2 \\ &- \left| \sum_{n=1}^\infty a_n \sin(nw + \phi_n) \right|^2 \Bigg]^2, \qquad \text{for } 0 < w < \pi. \end{aligned} \tag{13}$$

Once the unknown coefficients in (12) are known, the nonminimum phase function can be derived from

$$\begin{aligned} \Phi(w) &= \tan^{-1}\left[\frac{I(w)}{R(w)}\right] \\ &= \tan^{-1}\left[\frac{-\sum_{n=1}^\infty a_n \sin(nw + \phi_n)}{a_0 + \sum_{n=1}^\infty a_n \cos(nw + \phi_n)}\right]. \end{aligned} \tag{14}$$

The phase function $\Phi(w)$ associated with the amplitude $|X(w)|$ can indeed be either nonminimum or minimum phase, as no restrictions has been placed on its realization.

IV. Numerical Implementation

Since the numerical optimization process involved in (12) is highly time consuming, a good initial guess greatly improves the computation time. In order to achieve a good initial guess, we start with the power spectrum for $X(w)$ and generate from it the minimum-phase realization. We make sure that the function is defined between $0 < w < \pi$. Next, we utilize (1) to obtain the minimum phase response of the system, $\phi_{\min}(w)$. By utilizing the minimum-phase function, one can obtain an estimate of the real part of the transfer function as

$$R_{\min}(w) = |H(w)|\cos[\phi_{\min}(w)], \qquad \text{for } 0 < w < \pi. \tag{15}$$

We then obtain the discrete cosine transform of $R_{\min}(w)$ to obtain the coefficients $a_0, a_1, \cdots, a_N$, because of (10). The N coefficients a_i's are selected in such a way that the ratio of the maximum value of the coefficients to absolute value of a_N is equivalent to the number of effective digits available in the given data for the power spectrum (i.e., equivalent to the signal-to-noise ratio of the data).

The initial guess for all ϕ_n are set to zero and the optimization of (12) is carried out for the $2N+1$ unknown parameters

($N+1$ of a_i's and N of ϕ_i's). The computation of the series of a_i's during the error minimization iteration process can be done efficiently by utilizing the Fourier cosine transform and the sine transform. A point to note here is that it has been our experience that for a wide class of problems, the parameter ϕ_n has practically no influence on the optimization process for the a_i's and on the final solution (14). Hence, for most cases, it is necessary to compute only the $N+1$ coefficients of a_i.

V. Phase Synthesis of Far-Field Antenna Power Patterns

We know that the far field of an electromagnetic system is proportional to the Fourier transform of the current distribution. Since all antennas are of finite spatial size, this is equivalent to saying that the spatial current distribution is causal. Then, the real and imaginary parts of the magnetic vector potential are related by the Hilbert transforms because of the causal current distributions. Hence, given the magnitudes of the magnetic vector potentials (or the far fields power patterns they are related), one can utilize the principles presented earlier to generate the far-field phase pattern, which is often nonminimum phase.

Please note that for any current distributions, which are directed in the $\hat{z}$-direction and are expressed as

$$J_z(x, y, z)\begin{cases} x \in [-a; a] \\ z \in [-c; c] \\ y \in [-b; b] \end{cases} \tag{16}$$

the magnetic vector potential is given by

$$A_z = \frac{e^{-jkr}}{4\pi r}\int_{-a}^{a} dx \int_{-b}^{b} dy \int_{-c}^{c} dz\, J(x, y, z)\hat{z} \cdot \exp\left[jkx\sin\theta\sin\phi + jky\sin\theta\cos\phi + jkz\cos\theta\right] \tag{17}$$

where $k = \frac{2\pi}{\lambda}$ and r is the spatial far-field variable.

Hence, $A_z[\theta, \phi]$, or more exactly, $A_z[k\sin\theta\sin\phi; k\sin\theta\cos\phi; k\cos\theta]$ is the Fourier transform of the "causal" current distribution $J_z(x, y, z)$. For illustration purposes, we set $\phi = 0$. Further, we restrict the current distribution to the $y = 0$ plane (i.e., $b \equiv 0$), so that we have

$$A_z = \frac{e^{-jkr}}{4\pi r}\int_{-a}^{a} dx \int_{-c}^{c} dz\, J_z(x, z) e^{jkz\cos\theta} \tag{18}$$

and since the far field, $\mathbf{E} = -jw\mathbf{A}$, we have

$$E_\theta(\theta) = jw\sin\theta\, f_{un}(\theta) \tag{19}$$

where $f_{un}(\theta)$ are some functions of θ. Therefore, the real and the imaginary parts of A_z are related by the Hilbert transform. In general, we are given the power field patterns $|E_\theta(\theta)|^2$ and, hence, we transform the field patterns $E_\theta(\theta)$ to $A_z(\theta)$ by utilizing the following transformation:

$$E_\theta(\Omega) = j\sqrt{1-\Omega^2}\left(\sum_n a_n e^{-j(n\Omega+\phi_n)}\right)w \tag{20}$$

where $\Omega = \cos\theta$. The rationale of using (20) is that the real and imaginary parts of the magnetic vector potential are related by the Hilbert transform, but that does not apply to the fields, as is seen from (20).

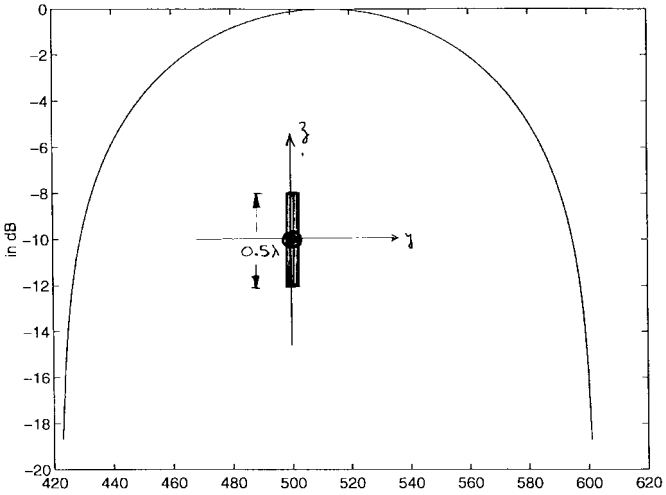

Fig. 1. Magnitude plot of the far field of a dipole antenna. $\omega = (x - 512)/128 \rightarrow x$.

In (20), we need to note that it is $\cos\theta$, not θ, which corresponds to the frequency variable Ω. The E-field data we get, in general, will be equispaced in θ-space, i.e., we will have $E_\theta(\theta)$ for $\theta = 0, 1^\circ, \cdots, 180^\circ$. However, the data we need in order to do optimization should be equispaced in $\cos\theta$ space, i.e., we should get the data in the form of $E_\theta(\cos\theta)$, $\cos\theta = -1, \cdots, 0, 1/N, 2/N, \cdots, 1$. Therefore, before we carry out the numerical optimization, we need to interpolate the data to make them equispaced in the $\cos\theta$ space. This is required for efficient computation of the series in (10) and (11) by the Discrete sine and the cosine transforms [6].

Finally, we need to know how to scale the data into $\omega\epsilon[-\pi, \pi]$. Because of the variation of $\cos\theta$, we can only get the data for $\Omega = \cos\theta\epsilon[-1, 1]$. However, if we consider the field pattern A_z as the Fourier transform of the current distribution, we will have the data for $\Omega\epsilon[-\infty, \infty]$. What we need to do is to scale the range of Ω from $[-\infty; \infty]$ to that of $\omega\epsilon[-\pi, \pi]$ for numerical computations [5].

Fortunately, for large Ω, the fields in the invisible region $A_z(\Omega)$ will become zero. Thus, if we can regard $A_z(\Omega) = 0$ for $|\Omega| > \Omega_0$, we can scale $\Omega\epsilon[-\Omega_0, \Omega_0]$ into $\omega\epsilon[-\pi, \pi]$ and then use (13) to perform the optimization. Also, we need to point out that by assuming $\Omega\epsilon[-1, 1]$ corresponding to $\omega\epsilon[-\omega_0, \omega_0]$, we only perform optimization in that range.

VI. Examples

As a first example, consider a half-wavelength long z-directed transmitting dipole of radius 0.001λ centered at the origin. The dipole is fed at the center with 1.0 V excitation. The magnitude response of the far field is given in Fig. 1. The x-axis is Ω. The region $-4 \leq \Omega \leq 4$ has been divided into 1024 subsections so that 512 is the value corresponding to $\Omega = 0$. The region $-1 \leq \Omega \leq 1$ then corresponds to 384 to 640 (i.e., $\Omega = x - 512/128$). The reconstructed phase utilizing the technique described in the paper is shown by a

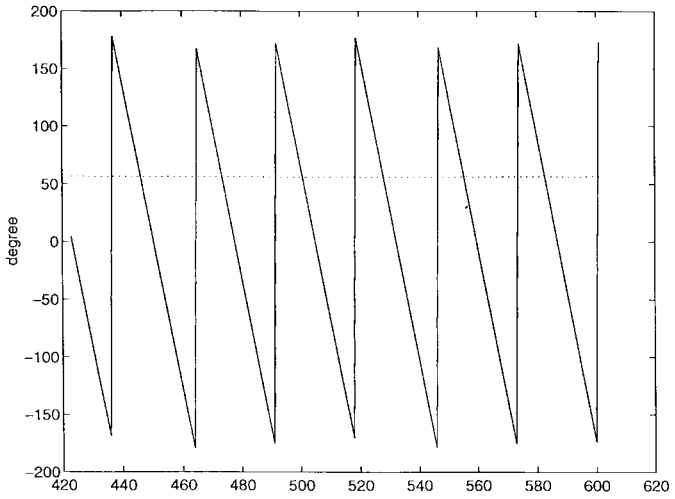

Fig. 2. Reconstructed phase (solid line) with the actual phase (dotted line) associated with Fig. 1. $\Omega = (x - 512)/128 \rightarrow x$.

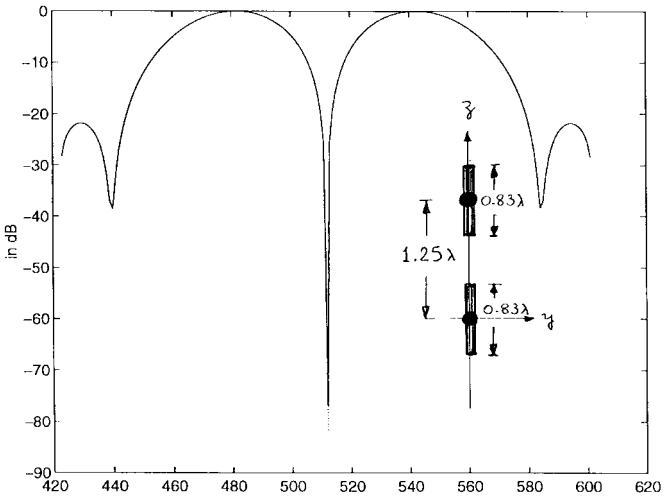

Fig. 4. Magnitude plot of the far field of two z-directed dipoles. $\omega = (x - 512)/128 \rightarrow x$.

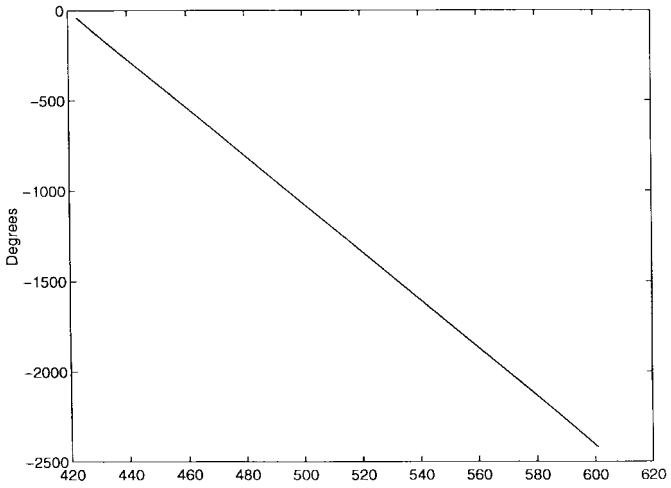

Fig. 3. Difference between the reconstructed phase and the actual phase. $\omega = (x - 512)/128 \rightarrow x$.

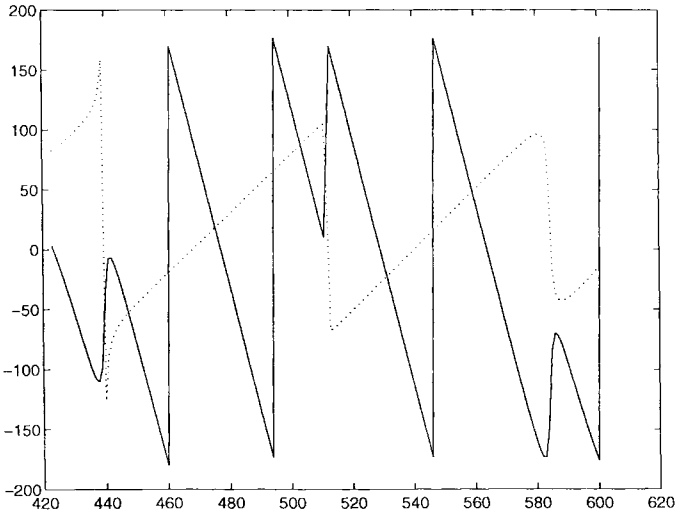

Fig. 5. Reconstructed phase (solid line) with the actual phase (dotted line) associated with Fig. 4. $\omega = (x - 512)/128 \rightarrow x$.

solid line in Fig. 2. Numerically, this has been accomplished by computing (14) utilizing the coefficients a_i and ϕ_j obtained from the minimization of the error function $E(w)$ in (13). The true phase calculated by the computer code analysis of wire antennas and scatterers (AWAS) [7] is shown by a dotted line. In Fig. 3, we show the difference between the true phase and the reconstructed nonminimum phase, and it is a straight line. This linear-phase function is due to the choice of the physical origin of the coordinate system for the half-wave dipole. The dipole is centered at the origin and, hence, is not strictly a "causal" function. The delay (linear-phase function) accounts for this spatial displacement of the origin.

For the second example, we consider two z-directed dipoles of lengths 0.83λ and radius 0.001λ, both oriented along the z-axis. One is centered at the origin and the other one is centered at 1.25λ away from the origin, so that they are separated by 0.42λ from end to end. Both the dipoles are center fed and excited with 1.0 V, but of opposite phase. The x-axis is Ω and it is given by $\Omega = (x - 512)/128$. The magnitude response is shown in Fig. 4, which has been computed using the AWAS code [7]. The true (dotted) and the reconstructed (solid) phase response is shown in Fig. 5. Again, if we observe the difference between the two phases in Fig. 6, note that it is almost a straight line, except for a couple of glitches. The glitches occur at pattern minimums which are 40 and 70 dB down and, hence, computation of phase by (14) becomes inaccurate as both the numerator and denominator values are small. However, since the pattern magnitudes are quite small, the glitches in the reconstructed phase is not a serious source of error.

As a third example, consider a three-element z-directed half-wave array of 0.001λ radius spaced a half-wavelength apart along the y-axis, all located in the $x = 0$ plane. All three elements are 0.5λ long and are excited with 1.0 V excitation. The magnitude-power pattern for the electric field $|E_\theta|$ for $\phi = 90°$ is given by Fig. 7, computed by the AWAS code. The scale of the x-axis in Fig. 7 is given by $\Omega = (x - 512)/128$.

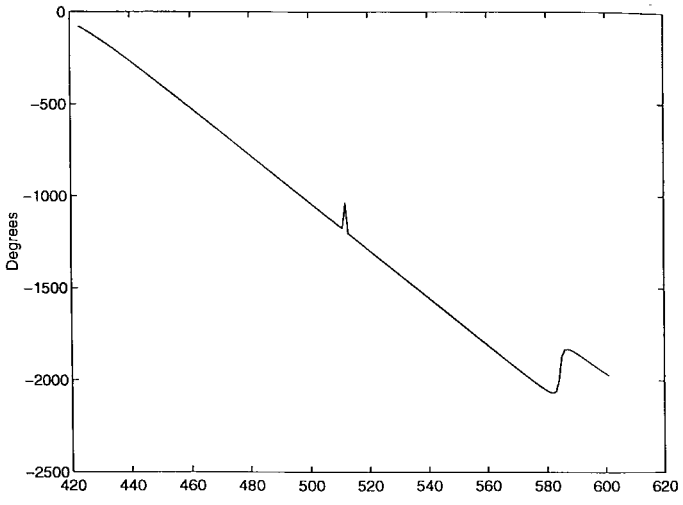

Fig. 6. Difference between the reconstructed phase and the actual phase. $\omega = (x - 512)/128 \rightarrow x$.

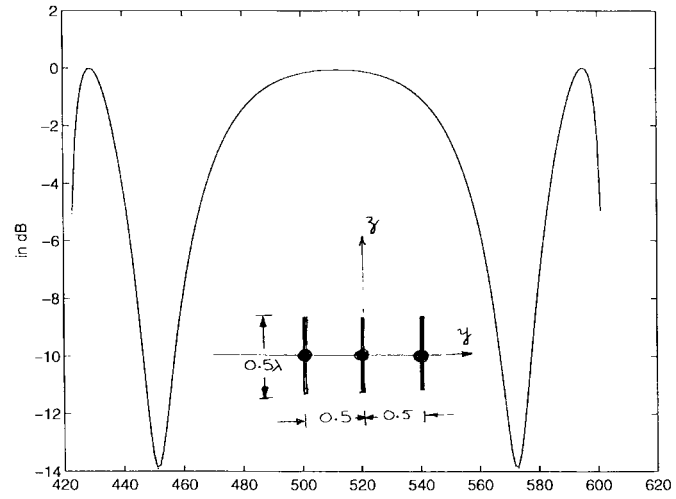

Fig. 7. Magnitude plot of the far field of three z-directed planar dipoles. $\omega = (x - 512)/128 \rightarrow x$.

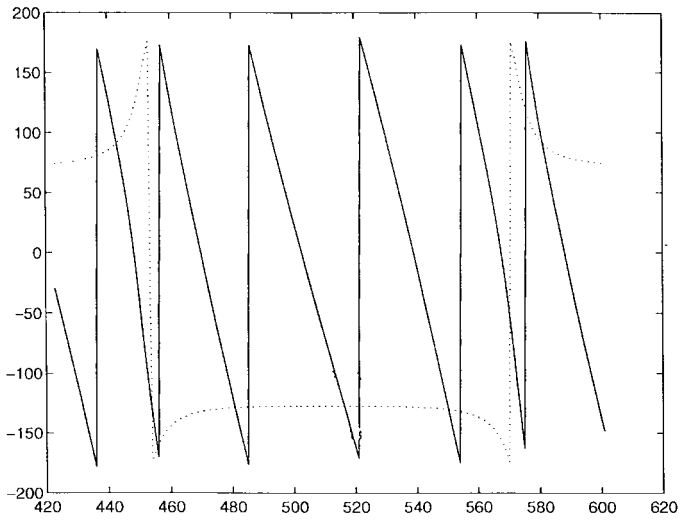

Fig. 8. Reconstructed phase (solid line) with the actual phase (dotted line) associated with Fig. 7. $\omega = (x - 512)/128 \rightarrow x$.

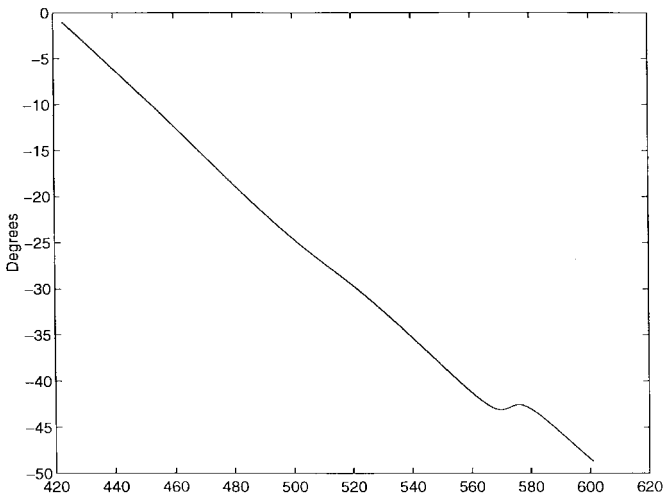

Fig. 9. Difference between the reconstructed phase and the actual phase. $\omega = (x - 512)/128 \rightarrow x$.

We need to note for this case, for $\phi = 90°$, the $f_{un}(\theta)$ in (19) is a function of $\cos\theta$, so we still can use the analysis presented earlier to do the optimization. In Fig. 8, the original phase, depicted by a dotted line, is displayed along with the reconstructed phase, shown by the solid line. Again, for both Figs. 8 and 9, the x-axis is $\Omega = (x - 512)/128$. In Fig. 9, it is seen that the difference between the two phases is almost a straight line. There is, however, a glitch in the linear-phase difference, again where the value of the pattern is minimum.

Finally, we test this theory on measured data. The experimental data consists of the s_{21}-parameter of a microwave bandpass filter measured in the band of 4.31 to 7.42 GHz at 256 equally spaced points. It is important to note that s_{21} is often a nonminimum phase function, whereas s_{11} is always minimum phase. The magnitude response is shown in Fig. 10. The x-axis corresponds to frequency, the origin corresponds to 3.532 GHz, and the plot extends to 8.19 GHz so that $f = (x \times 0.7775) + 3.5325$ GHz. The measured s_{21}-response below -10 dB is discarded along with the phase. The actual

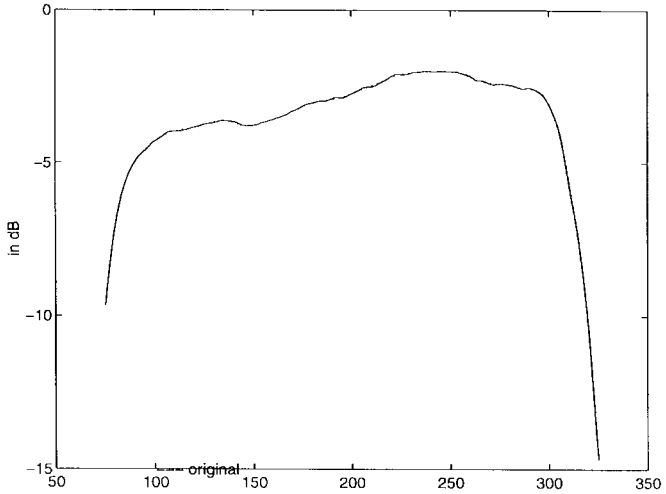

Fig. 10. Magnitude response of the s_{21}-parameter of a filter. $f = 3.53 + 0.7775^{*}x \rightarrow x$.

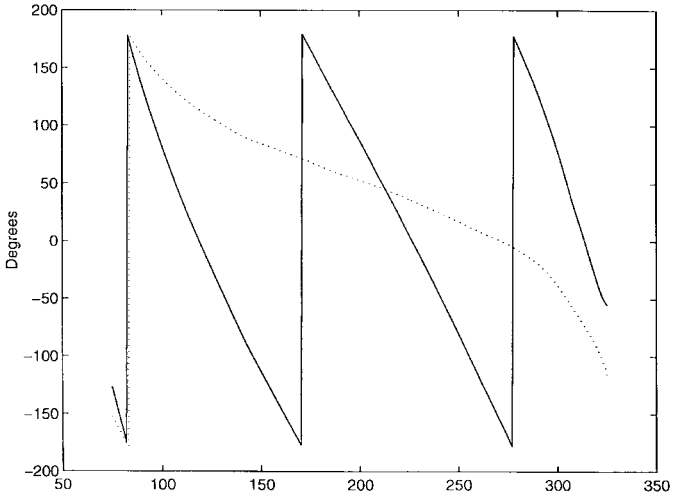

Fig. 11. Reconstructed phase (solid line) with the actual phase (dotted line) associated with Fig. 10. $f = 3.53 + 0.7775^{*}x \rightarrow x$.

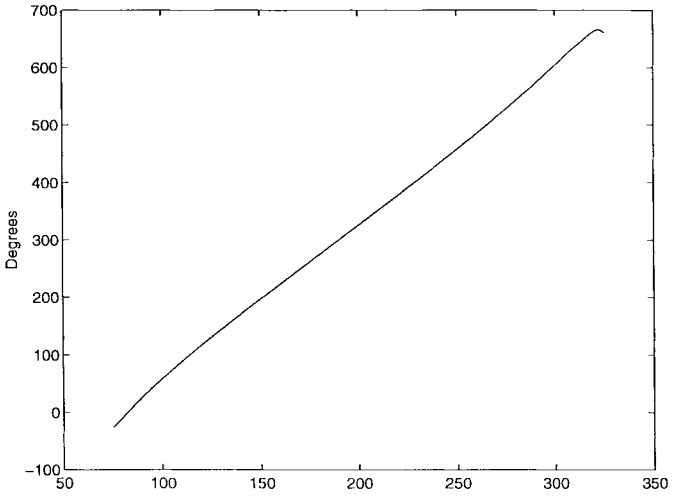

Fig. 12. Difference between the reconstructed phase and the actual phase. $f = 3.53 + 0.7775^{*}x \rightarrow x$.

phase (dotted line) and the reconstructed phase (solid line) is shown in Fig. 11. Fig. 12 provides the difference between the two, which again is similar to a linear phase.

For all the examples described here, the initial starting guess was the minimum-phase response for the phase function, and they are no where near the true solution. Also, the difference between the reconstructed and the true phase function is always a linear phase, as we do not have any information about how much delay the system introduces to the input function. The magnitude response contains only the information about the power density.

VII. Conclusion

A method based on the Hilbert-transform technique is outlined to generate the nonminimum phase function of electromagnetic systems. Currently work is under way to extend the formulation to the multidimensional case.

References

[1] G. C. James, "Phase retrieval and near field antenna measurements," in *Proc. URSI Symp.*, Sydney, Australia, 1992, pp. 510–512.

[2] Y. M. Bruck and L. G. Sodin, "On the ambiguity of the image reconstruction problem," *Opt. Commun.*, vol. 30, no. 3, Sept. 1979, pp. 304–308.

[3] M. H. Hayes, "The reconstruction of a multidimensional sequence from the phase or magnitude of its Fourier transform," *IEEE Trans. Acoust., Speech, Signal Processing*, vol. ASSP-30, pp. 140–154, Apr. 1982.

[4] A. D. Poularikas, *The Transforms and Applications Handbook.* Piscataway, NJ: IEEE Press, 1996.

[5] A. V. Oppenheim and R. W. Schafer, *Discrete-Time Signal Processing*. 2nd ed. Englewood Cliffs, NJ: Prentice-Hall, 1989, chs. 5 and 10.

[6] S. Narayana *et al.*, "A comparison of two techniques for the interpolation extrapolation of frequency domain responses," *Digital Signal Processing*, vol. 6, pp. 51–67, 1966.

[7] A. R. Djordjevic *et al.*, *Analysis of Wire Antennas and Scatterers.* Norwood, MA: Artech House, 1990.

[8] S. Narayana, S. M. Rao, R. Adve, T. K. Sarkar, V. C. Vannicola, M. Wicks, and S. Scott, "Interpolation/extrapolation of frequency responses using the Hilbert transform," *IEEE Trans. Microwave Theory Tech.*," vol. 44, pp. 1621–1627, Oct. 1996.

Tapan K. Sarkar (S'69–M'76–SM'81–F'92) received the B.Tech. degree from the Indian Institute of Technology, Kharagpur, India, the M.Sc.E. degree from the University of New Brunswick, Fredericton, Canada, in 1969, and the M.S. and Ph.D. degrees from Syracuse University, Syracuse, NY, in 1971 and 1975, respectively.

From 1975 to 1976, he was with the TACO Division, General Instruments Corporation. From 1976 to 1985, he was with the Rochester Institute of Technology, Rochester, NY. From 1977 to 1978, he was a Research Fellow at the Gordon McKay Laboratory, Harvard University, Cambridge, MA. He is currently a Professor in the Department of Electrical and Computer Engineering, Syracuse University. He has authored or co-authored over 154 journal articles and conference papers and has written chapters in eight books. His current research interests deal with numerical solutions of operator equations arising in electromagnetics and signal processing with application to system design.

Dr. Sarkar is a Registered Professional Engineer in the State of New York. He is a member of Sigma Xi and the International Union of Radio Science Commissions A and B. He was an associate editor for feature articles of the *IEEE Antennas and Propagation Society Newsletter*. He was the technical program chairman for the 1988 IEEE AP-S International Symposium and URSI Radio Science Meeting, and has been appointed U.S. research council representative to many URSI General Assemblies. He is the chairman of the Intercommission Working Group of International URSI on Time-Domain Metrology. He received one of the "Best Solution" Awards in 1977, presented at the Rome Air Development Center (RADC) Spectral Estimation Workshop, and the Best Paper Award of the IEEE TRANSACTIONS ON ELECTROMAGNETIC COMPATABILITY in 1979.

Bin Hu, photograph and biography not available at the time of publication.